Current **A**pplied **S**cience and **T**echnology e-ISSN: 2586-9396

Curr. Appl. Sci. Technol. ….., Vol... (No...), e0268210

Research article

Influence of Annealing Atmospheres on the Structural and Thermoelectric Characteristics of Sb_2Te_3 Thin Film

Khunnapat Sriporaya[1], Mati Horprathum[2] Athorn Vora-ud[3], Saksorn Limwichean[2] and Nat Kasayapanand[1]*

[1]Energy Technology Program, School of Energy Environment and Materials, King Mongkut's University of Technology Thonburi 126 Pracha Uthit Rd., Bang Mod, Thung Khru, Bangkok, 10140, Thailand
[2]National Electronics and Computer Technology Center, 114 Thailand Science Park, Paholyothin Road, Klong 1, Klong Luang, Pathumthani 12120, Thailand
[3]Program of Physics, Faculty of Science and Technology, Sakon Nakhon Rajabhat University, 680 Nittayo Road, Mueang District, Sakon Nakhon 47000, Thailand

Received: 2 July 2025, Revised: 9 October 2025, Accepted: 23 October 2025, Published: 10 April 2026

Abstract

Antimony telluride (Sb_2Te_3) thin films were deposited on 1-μm SiO_2 / Si-wafer substrates to a thickness of approximately 250 nm by using pulse-dc magnetron sputtering method, and their thermoelectric (TE) properties were evaluated. This study examined the impact of post-annealing at 250°C under vacuum, argon (Ar), and nitrogen (N_2) atmospheres on the thermoelectric (TE) properties. The surface morphology, crystalline structure, and atomic composition were analyzed for both as-deposited and post-annealed thin films using field emission scanning electron microscopy (FE-SEM), grazing incidence X-ray diffraction (GI-XRD) and energy dispersive X-ray spectroscopy (EDS), respectively. The results revealed that post-annealing significantly influenced the thin film structure, enhancing the Sb_2Te_3 crystal orientations, particularly the (015) and (10$\bar{1}$0) peaks. Additionally, Hall effect measurement performed after post-annealing confirmed the electrical properties of all samples, providing further understanding of their electrical properties. For the thermoelectric (TE) properties, low temperature Seebeck coefficient analysis confirmed the p-type character of Sb_2Te_3. The argon post-annealed sample exhibited the highest Seebeck coeefficient of 1.0 x 10^{-4} V/K, corresponding to a maximum power factor (PF) of 4.40 x 10^{-4} W/m K^{-2}. The results clearly show that post-annealing temperature directly affected both the electrical and thermoelectric characteristics.

Keywords: Sb_2Te_3 thin films; magnetron sputtering; post-annealing; thermoelectric

*Corresponding author: E-mail: nat.kas@kmutt.ac.th
https://doi.org/10.55003/cast.2026.268210
Copyright © 2024 by King Mongkut's Institute of Technology Ladkrabang, Thailand. This is an open access article under the CC BY-NC-ND license (http://creativecommons.org/licenses/by-nc-nd/4.0/).

1. Introduction

In recent years, environmentally friendly, portable, and wearable electronic devices capable of self-generating electrical power have attracted significant attention (Wang et al., 2020; Zhang et al.,2021). These devices offer considerable advantages for advancing the Internet of Things (IoT) ecosystem and wearable technology applications (Lopera et al., 2016; Dunham et al., 2018). Among various energy-harvesting approaches, microscale thermoelectric generators (μTEGs) based on thin-film technologies have emerged as a promising solution due to their compact size, flexibility, and ability to convert body or ambient heat into electricity (Dunham et al., 2018; Snyder et al., 2021). The performance of thermoelectric (TE) materials is generally evaluated using the dimensionless figure of merit, ZT, defined as $ZT = (S^2\sigma T)/\kappa$ and power factor; $PF = S^2\sigma$, where S is the Seebeck coefficient (V/K), σ is the electrical conductivity (S/m), T is the absolute temperature (K), and κ is the thermal conductivity (W/m·K) (Jiang et al., 2021, Tan et al., 2021).

A great deal of research has been devoted to the development of TE materials with enhanced ZT values, and various compounds such as Bi_2Te_3 (Chung et al., 2000), Si,Ge,Sn (Lan et al., 2010), PbTe/PbS (Li et al., 2013), SnTe (Moshwan et al., 2017), and Sb_2Te_3 (Hong et al., 2014) have been reported as promising candidates. It is well established that the most efficient TE materials for room-temperature applications are narrow band-gap semiconductors (Eg < 0.2 eV at room temperature) (Hong et al., 2014). Among these, Sb_2Te_3 is widely recognized as a favorable p-type thermoelectric material, owing to its high ZT value at room temperature and narrow band-gap energy (~0.14 eV) (Olson et al., 2006). These properties make Sb_2Te_3 an attractive choice for μTEGs. Sb_2Te_3 thin films have been fabricated using various techniques, including thermal evaporation (Zou et al., 2001), magnetron sputtering (Kim et al., 2006), pulsed laser deposition (Giani et al.,1999), and metal-organic chemical vapor deposition (Makala et al., 2003). Among these methods, magnetron sputtering is widely used for commercial thin-film deposition due to its process stability, reproducibility, and high efficiency, which enable the production of high-quality films (Lee et al., 2012). However, a common limitation of the sputtering technique is its low ionization efficiency, which often leads to poor crystallinity and reduced electrical performance in as-deposited films.

To overcome these limitations, previous studies have employed post-annealing treatments in different atmospheres such as vacuum (Fan et al., 2010), nitrogen (N_2) (Fang et al., 2013), and argon (Ar) (Hong et al., 2014) following deposition. These treatments aim to enhance the film's stoichiometry and thermoelectric performance (Fang et al., 2013). Despite these efforts, a comprehensive and systematic comparison of the effects of different annealing atmospheres on the structural and thermoelectric properties of Sb_2Te_3 thin films has not yet been fully explored in the literature.

In this study, we systematically investigate the effects of post-annealing in three different atmospheres vacuum, N_2, and Ar on the properties of Sb_2Te_3 thin films deposited by pulse-dc magnetron sputtering onto SiO_2 substrate. The aim is to explore how each annealing environment influences the microstructural characteristics, electrical conductivity, and thermoelectric performance of the films. A deeper understanding of these effects is crucial for optimizing the fabrication process and improving the overall performance of Sb_2Te_3 thin films for future thermoelectric (TE) applications, particularly in compact and energy-harvesting devices.

2. Materials and Methods

2.1 Materials and Methods

Sb_2Te_3 thin films were fabricated using the pulse-dc magnetron sputtering method (ATC 2000-F, AJA International, Inc.). The deposition was caried out on 1-μm SiO_2 / Si-wafer substrates using a Sb:Te; 2:3 ratio target of 99.99% purity with 2-inch diameter and 0.25-inch thickness. Sputtering was performed under a base pressure of 5.0×10^{-6} mbar and a working pressure of about 3.0×10^{-3} mbar using argon gas (99.999%) at flow rate of 20 sccm. The pulsed-dc sputtering power of the Sb_2Te_3 target was fixed at 25 W. The deposition time was maintained for 35 min with thin film deposited to a thickness of approximately 250 nm. After fabrication, the as-deposited thin films were annealed at temperature 250°C for 30 min under different atmospheric conditions, which were vacuum annealing under pressure of 3.0×10^{-2} mbar, argon annealing, and nitrogen annealing (99.999%) under pressure of 1.0×10^{-1} mbar. This post-annealing process was carried out to investigate the influence of annealing environment on the structural and thermoelectric properties of the Sb_2Te_3 thin films.

2.2 Characterizations

The surface morphologies, crystalline structure, and chemical composition of all Sb_2Te_3 thin films conditions were investigated by field emission scanning electron microscope (FE-SEM; Hitachi SU8030), grazing Incidence X-ray diffraction (GI-XRD; TTRAX III-Rigaku) and energy dispersive spectroscopy (EDS), respectively. Moreover, the carrier concentration (n), mobility (μ), and electrical resistivity (ρ) were investigated by Hall effect measurement (HMS-3000, Ecopia) using a magnetic field of 0.55 T at room temperature. Finally, electrical resistivity (ρ), Seebeck coefficient (S), and power factor (PF) of the Sb2Te3 thin films annealed in all atmospheres were measured by a ZEM-3 apparatus (Advance Riko) under an applied temperature range of room temperature to 200°C.

3. Results and Discussion

Figure 1 shows the FE-SEM images of the Sb_2Te_3 thin films deposited by pulse-dc magnetron sputtering and the as-deposited sample with films post-annealed at 250°C in different atmospheres (vacuum, N_2, and Ar) were compared. From the top-view SEM images, the as-deposited film exhibits densely packed, fine grains, while all post-annealed samples display slightly coarser grains with increased intergranular spacing. This morphological evolution suggests grain growth and microstructural reorganization induced by the annealing process (Hong et al., 2014). The cross-sectional SEM images show that all films have relatively similar thicknesses. The as-deposited film has a thickness of 263±5 nm, and a slight decrease in thickness is observed for all annealed films regardless of the annealing atmosphere. This reduction may be attributed to film densification and atomic rearrangement resulting from the thermal treatment (Zheng et al., 2013; Thaowonkaew et al., 2021). The crystallinity of the Sb_2Te_3 thin films, both as-deposited and post-annealed in three different atmospheres, was investigated using grazing incidence X-ray diffraction (GI-XRD), as shown in Figure 2. The XRD patterns confirm the formation of a polycrystalline Sb_2Te_3 phase in all samples, with the main diffraction peaks corresponding to the (015) and $(10\bar{1}0)$ planes located at 2θ values of 28.24° and 38.29°, respectively. These reflections are consistent with the rhombohedral crystal structure of Sb2Te3

(JCPDS No. 15-0874) (Takayama & Takashiri, 2017). The as-deposited film exhibits relatively broad and low-intensity peaks, indicative of poor crystallinity. Upon post-annealing, the diffraction peaks become sharper and more intense, particularly for the sample annealed in argon, suggesting a significant enhancement in crystallinity. This improvement can be attributed to the increased thermal energy provided during annealing, which facilitates atomic diffusion, grain agglomeration, and structural reordering into a more crystalline phase (Duan & Jiang, 2010; Liu et al., 2015; Somdock et al., 2019). Among the annealed samples, the film treated in argon exhibits the most pronounced (015) peak, indicating a preferred orientation along this plane and superior crystallinity compared to those annealed in vacuum and nitrogen.

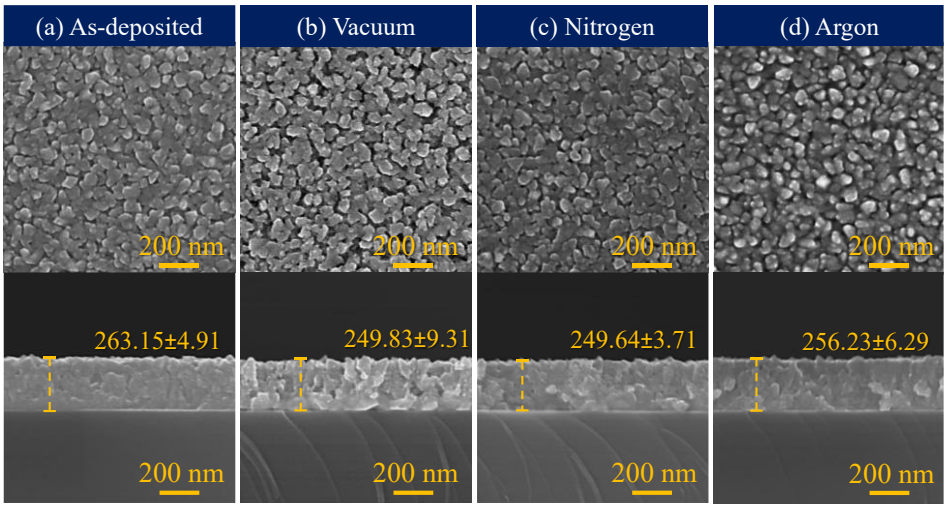


Figure 1. FE-SEM images of Sb_2Te_3 thin films (a) as-deposited, (b-d) post-annealed in in vacuum, nitrogen, and argon atmospheres, respectively

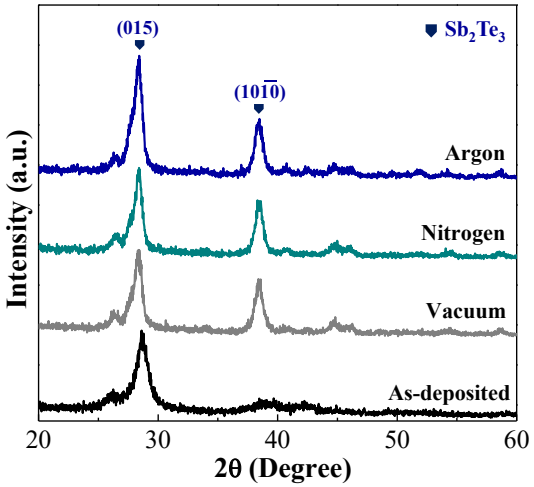


Figure 2. The crystallinity by XRD of Sb_2Te_3 thin films, both as-deposited and post-annealed in all atmospheres

As shown in Figure 3, energy-dispersive X-ray spectroscopy (EDS) was employed to analyze the elemental composition of Sb_2Te_3 thin films in both the as-deposited state and after post-annealing in various atmospheres. Figure 3(a) displays the EDS spectra, which clearly shows the presence of Sb and Te as the primary elements, as expected. Peaks corresponding to Si from the underlying silicon substrate were also detected in all samples, along with Al, which originates from the supporting stage used during analysis. Additionally, C and O signals were observed across all spectra, attributed to surface contamination and partial oxidation of the film surface during or after deposition (Chaiwas et al., 2024). The atomic composition (at%) results are summarized in Figure 3(b). The as-deposited film exhibited an Sb content of 35.23%, which increased slightly after post-annealing in all atmospheres, ranging from 36.71% to 39.83%. In contrast, the Te content showed a corresponding decrease from 64.76% in the as-deposited film to 60.16% after annealing. This trend is consistent with previous studies and is attributed to the re-evaporation of the more volatile Te element during the annealing process, particularly at elevated temperatures (Zheng et al., 2013). In addition, the calculated Sb/Te atomic ratios were found to be 0.54 (as-deposited), 0.66 (vacuum-annealed), 0.58 (Ar-annealed), and 0.64 (N_2-annealed), respectively. These results indicate that annealing leads to a composition closer to the stoichiometric ratio (Sb:Te = 2:3), suggesting improved film quality and better control over elemental balance through post-annealing treatments.

The electrical properties of the Sb_2Te_3 thin films were characterized using Hall effect measurements, as presented in Figure 4. The measured parameters included carrier concentration (cm^3), carrier mobility ($cm^2/V{\cdot}s$), and electrical resistivity ($\Omega{\cdot}cm$). As shown in Figure 4(a), the carrier concentration of the as-deposited film was relatively low, approximately 1.10×10^{18} cm^3, but increased significantly after post-annealing, reaching values in the range of 1.60 to 2.00×10^{18} cm^3. This increase is attributed to changes in atomic composition caused by thermal annealing, consistent with previous studies (Takayama & Takashiri, 2017). The enhancement in carrier concentration also contributed to a marked improvement in carrier mobility, which increased from 2.40 $cm^2/V{\cdot}s$ in the as-

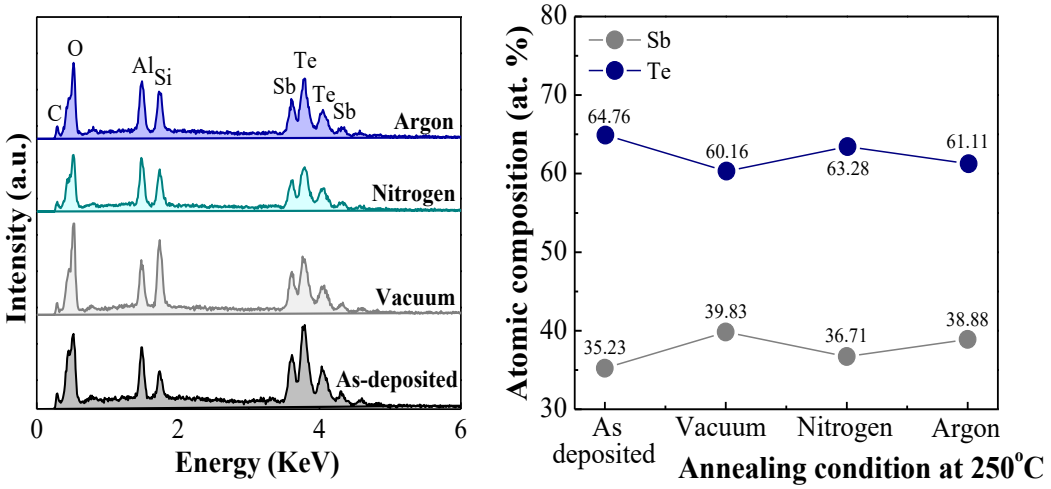


Figure 3. (a) The EDS spectra of Sb_2Te_3 both as-deposited and post-annealed condition and (b) atomic composition of Sb and Te value in all.

deposited sample to as high as 29.0 $cm^2/V{\cdot}s$ in the post-annealed films. Figure 4(b) illustrates the corresponding change in electrical resistivity, which decreased significantly following annealing. The as-deposited film exhibited a resistivity of 6.0×10^{-2} Ω·cm, which dropped to $3.40 – 3.20 \times 10^{-3}$ Ω·cm after annealing in all atmospheres. This reduction in resistivity can be attributed to the improved crystallinity and increased carrier mobility achieved through thermal treatment, leading to enhanced electrical transport properties (Rimoldi et al., 2021).

Finally, the thermoelectric properties including electrical resistivity (Ω/m), Seebeck coefficient (V/K), and power factor ($W/m{\cdot}K^2$) were evaluated using a ZEM-3 system over the applied temperature range of 50-200°C, as shown in Figure 5. In Figure 5(a), the film annealed in argon atmosphere exhibits remarkably stable resistivity, maintaining a value of approximately 2.40×10^{-5} Ω/m across the entire temperature range. In contrast, the resistivity of the films annealed in vacuum and nitrogen shows a decreasing trend with increasing temperature, which is typical semiconductor behavior. The stable resistivity after argon annealing results from the amorphous-to-crystalline transition, which reduces defect density and charge carrier scattering. Enhanced crystallinity and fewer vacancy-related scattering centers collectively stabilize the electrical transport behavior (Snyder & Toberer, 2008; Goldsmid, 2010; Prainetr et al., 2020). As shown in Figure 5(b), the Seebeck coefficient (S) for all samples decreases with increasing temperature. The vacuum-annealed film exhibits the highest positive Seebeck coefficient at low temperatures, suggesting dominant p-type conduction. However, above 150°C, the Seebeck coefficient becomes negative for all samples, indicating a transition from p-type to n-type conduction. This behavior is consistent with the properties of narrow band-gap semiconductors like Sb_2Te_3, where thermal excitation promotes intrinsic carrier generation and results in a shift in the dominant carrier type due to an imbalance between electrons and holes (Prainetr et al., 2020). Figure 5(c) presents the calculated power factor ($PF = S^2\sigma$), which represents the overall thermoelectric performance. At 50°C, the power factor reaches approximately 4.40×10^{-4}, 3.10×10^{-4}, and 2.30×10^{-4} $W\ m^{-1}K^{-2}$ for the films annealed in argon, vacuum, and nitrogen, respectively. This result indicates that argon annealing offers the most

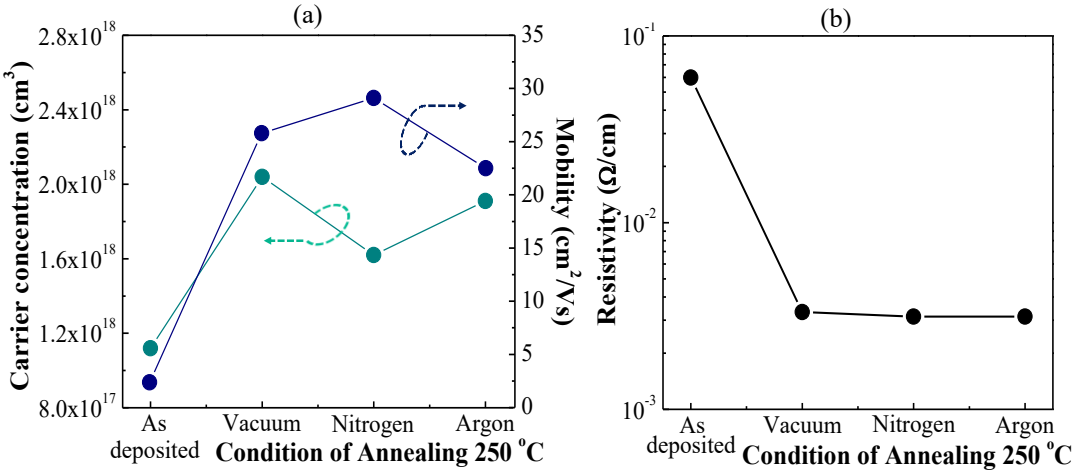


Figure 4. The electrical properties of thin films both as-deposited and post-annealed in all atmospheres (a) carrier concentration and mobility and (b) resistivity

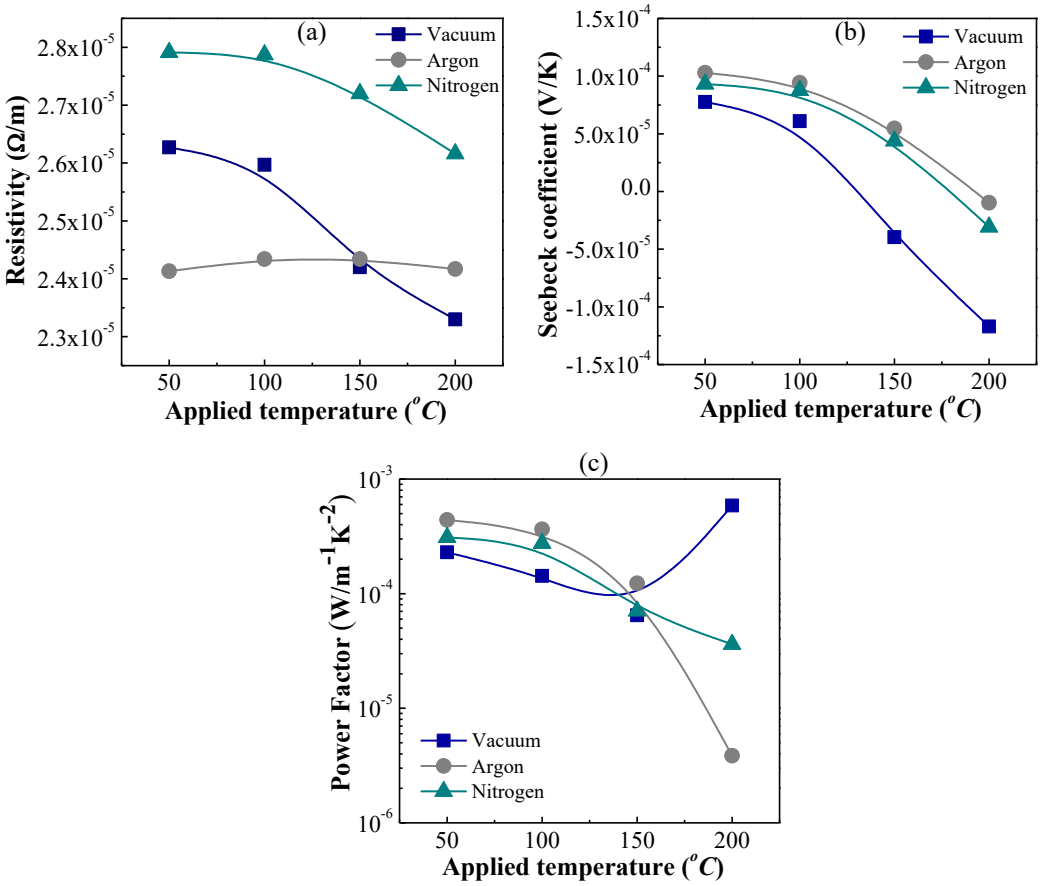


Figure 5. The thermoelectric properties of Sb_2Te_3 in all condition (a) resistivity (b) Seebeck coefficient and (c) power factor

favorable thermoelectric performance at low temperatures. However, the power factor of all samples decreases significantly at higher temperatures due to the combined effects of the declining Seebeck coefficient and the instability of conduction type. These findings suggest that the Sb_2Te_3 thin films prepared in this study are most suitable for low-temperature thermoelectric applications, as their performance degrades at elevated temperatures and undergoes a conduction-type transition, which can adversely affect device stability.

4. Conclusions

In this study, Sb_2Te_3 thin films were successfully fabricated using pulse-dc magnetron sputtering on SiO_2/Si substrates, followed by post-annealing in three different atmospheres: vacuum, nitrogen, and argon. The effects of annealing conditions on the structural, electrical, and thermoelectric properties of the films were systematically investigated. The results showed that post-annealing significantly enhanced the

crystallinity and electrical performance of the films compared to the as-deposited state. Among the films annealed under different atmospheres, the argon annealed films exhibited the most stable resistivity, near-stoichiometric composition, and superior power factor at low temperatures. This behavior was attributed to improved microstructural quality and reduced Te volatilization during annealing. Temperature-dependent Seebeck measurements revealed a p-type to n-type conduction transition above 150°C in all samples, consistent with the behavior of narrow band-gap semiconductors. The overall thermoelectric performance, particularly the power factor, was highest at 50°C for the argon-annealed sample, highlighting its suitability for low-temperature thermoelectric applications. These findings underscore the importance of annealing atmosphere in tuning the thermoelectric properties of Sb_2Te_3 thin films and suggest that argon annealing provides an effective route for optimizing performance in microscale or wearable thermoelectric devices.

5. Acknowledgements

This work was supported by Thailand Science Research and Innovation (TSRI), and National Science, Research, and Innovation Fund (NSRF) Fiscal year 2024 Grant number (FRB670016/0164). We acknowledge the support from Faculty of Energy, Environment and Materials, School of Energy Technology, King Mongkut's University of Technology of Thonburi (KMUTT), National Electronics and Computer Technology Center (NECTEC), Thailand. The authors are likewise grateful to Opto-Electrochemical Sensing Research Team, Spectroscopic and Sensing Devices Research Group, NECTEC and Program of Physics, Faculty of Science and Technology Sakon Nakhon Rajabhat University (SNRU) for experimental of thermoelectric.

6. Authors' Contributions

Khunnapat Sriporaya: analyzed data, writing – original draft, Investigation and formal analysis. Mati Horprathum: validation and supervision. Athorn Vora-ud: resources and methodology. Saksorn Limwichean: writing – review and editing, designed research, conceptualization and methodology Nat Kasayapanand: coordinated research, funding acquisition and supervision.

7. Conflicts of Interest

The authors declare no conflict of interest.

References

Chaiwas, S., Kasayapanand, N., Vora-ud, A., Chananonnawathorn, C., Kowong, R., Limwichean, S., Wongdamnern, N., Nakajima, H., & Horprathum, M. (2024). Enhanced thermoelectric power factor of magnetron co-sputtered Pd-added Bi_2Te_3 thin films. *Vacuum*, *230*, Article 113696. https://doi.org/10.1016/j.vacuum.2024.113696

Chung, D. Y., Hogan, T., Brazis, P., Rocci-Lane, M., Kannewurf, C., Bastea, M., Uher, C., & Kanatzidis, M. G. (2000). $CsBi_4Te_6$: A high-performance thermoelectric material for low-temperature applications. *Science*, *287*(5455), 1024-1027. https://doi.org/10.1126/science.287.5455.1024

Duan, X., & Jiang, Y. (2010). Annealing effects on the structural and electrical transport properties of n-type $Bi_2Te_{2.7}Se_{0.3}$ thin films deposited by flash evaporation. *Applied Surface Science*, *256*(24), 7365-7370. https://doi.org/10.1016/j.apsusc.2010.05.069

Dunham, M. T., Barako, M. T., Cornett, J. E., Gao, Y., Haidar, S., Sun, N., Asheghi, M., Chen, B., & Goodson, K. E. (2018). Experimental characterization of microfabricated thermoelectric energy harvesters for smart sensor and wearable applications. *Advanced Materials Technologies*, *3*, Article 1700383. https://doi.org/10.1002/admt.201700383

Fan, P., Zheng, Z.-H., Liang, G.-X., Zhang, D.-P., & Cai, X.-M. (2010). Thermoelectric characterization of ion beam sputtered Sb_2Te_3 thin films. *Journal of Alloys and Compounds*, *505*(1), 278-280. https://doi.org/10.1016/j.jallcom.2010.06.046

Fang, B., Zeng, Z., Yan, X., & Hu, Z. (2013). Effects of annealing on thermoelectric properties of Sb_2Te_3 thin films prepared by radio frequency magnetron sputtering. *Journal of Materials Science: Materials in Electronics*, *24*, 1105-1111. https://doi.org/10.1007/s10854-012-0832-4

Giani, A., Boulouz, A., Pascal-Delannoy, F., Foucaran, A., Charles, E., & Boyer, A. (1999). Growth of Bi_2Te_3 and Sb_2Te_3 thin films by MOCVD. *Materials Science and Engineering: B*, *64*(1), 19-24. https://doi.org/10.1016/S0921-5107(99)00142-7

Goldsmid, H. J. (2010). *Introduction to thermoelectricity*. Springer. https://doi.org/10.1007/978-3-642-00716-3

Hong, J.-E., Lee, S.-K., & Yoon, S.-G. (2014). Enhanced thermoelectric properties of thermal treated Sb_2Te_3 thin films. *Journal of Alloys and Compounds*, *583*(15), 111-115. https://doi.org/10.1016/j.jallcom.2013.08.164

Jiang, C., Wei, P., Ding, Y., Cai, K., Tong, L., Gao, Q., Lu, Y., Zhao, W., & Chen, S. (2021). Ultrahigh performance polyvinylpyrrolidone/Ag_2Se composite thermoelectric film for flexible energy harvesting. *Nano Energy*, *80*, Article 105488. https://doi.org/10.1016/j.nanoen.2020.105488

Kim, D.-H., Byon, E., Lee, G.-H., & Cho, S. (2006). Effect of deposition temperature on the structural and thermoelectric properties of bismuth telluride thin films grown by co-sputtering. *Thin Solid Films*, *510*(1-2), 148-153. https://doi.org/10.1016/j.tsf.2005.12.306

Lan, Y., Minnich, A. J., Chen, G., & Ren, Z. (2010). Enhancement of thermoelectric figure-of-merit by a bulk nanostructuring approach. *Advanced Functional Materials*, *20*, 357-376. https://doi.org/10.1002/adfm.200901512

Lee, H.-J., Park, H. S., Han, S., & Kim, J. Y. (2012). Thermoelectric properties of n-type Bi–Te thin films with deposition conditions using RF magnetron co-sputtering. *Thermochimica Acta*, *542*, 57-61. https://doi.org/10.1016/j.tca.2012.01.003

Li, J. Q., Li, X. X., Liu, F. S., Ao, W. Q., & Li, H. T. (2013). Enhanced thermoelectric properties of $(PbTe)_{0.88}(PbS)_{0.12}$ composites by Sb doping. *Journal of Electronic Materials*, *42*(1), 366-371

Liu, T., Deng, H., Cao, H., Zhou, W., Zhang, J., Liu, J., Yang, P., & Chu, J. (2015). Structural, optical and electrical properties of Sb_2Te_3 films prepared by pulsed laser deposition. *Journal of Crystal Growth*, *416*, 78-81. https://doi.org/10.1016/j.jcrysgro.2015.01.022

Lopera, J. M., del Arco Rodríguez, H., Pereira, J. M. P., de Castro, A. R., & Vigil, J. L. R. (2016). Wireless sensors supplied by energy harvesting thermoelectric generators. In *IEEE Industry Applications Society Annual Meeting* (pp. 1-8). IEEE. https://doi.org/10.1109/IAS.2016.7731916

Makala, R. S., Jagannadham, K., & Sales, B. C. (2003). Pulsed laser deposition of Bi_2Te_3-based thermoelectric thin films. *Journal of Applied Physics*, *94*(6), 3907-3918. https://doi.org/10.1063/1.1600524

Moshwan, R., Yang, L., Zou, J., & Chen, Z.-G. (2017). Eco-friendly SnTe thermoelectric materials: Progress and future challenges. *Advanced Functional Materials*, *27*(47), Article 1703278. https://doi.org/10.1002/adfm.201703278

Olson, J. K., Li, H., Ju, T., Viner, J. M., & Taylor, P. C. (2006). Optical properties of amorphous GeTe: The role of oxygen. *Journal of Applied Physics*, *99*, Article 103508. https://doi.org/10.1063/1.2194327

Prainetr, N., Vora-ud, A., Horprathum, M., Muthitamongkol, P., Thaowonkaew, S., Santhaveesuk, T., Phan, T. B., & Seetawan, T. (2020). Transfer of P-type to N-type thermoelectric properties of Ag–Sb–Te thin film through temperature annealing and its electrical power generation. *Journal of Electronic Materials*, *49*, 572-577. https://doi.org/10.1007/s11664-019-07756-9

Rimoldi, M., Cecchini, R., Wiemer, C., Longo, E., Cecchi, S., Mantovan, R., & Longo, M. (2021). Effect of substrates and thermal treatments on metalorganic chemical vapor deposition-grown Sb_2Te_3 thin films. *Crystal Growth and Design*, *21*, 5135-5144.

Snyder, G. J., & Toberer, E. S. (2008). Complex thermoelectric materials. *Nature Materials*, *7*, 105-114. https://doi.org/10.1038/nmat2090

Somdock, N., Kianwimol, S., Harnwunggmoung, A., Sakulkalavek, A., & Sakdanuphab, R. (2019). Simultaneous stoichiometric composition and highly (00l) orientation of flexible Bi_2Te_3 thin films via optimising the DC magnetron sputter-deposition process. *Journal of Alloys and Compounds*, *773*, 78-85. https://doi.org/10.1016/j.jallcom.2018.09.216

Takayama, K., & Takashiri, M. (2017). Multi-layered-stack thermoelectric generators using p-type Sb_2Te_3 and n-type Bi_2Te_3 thin films by radio-frequency magnetron sputtering. *Vacuum*, *144*, 164-171. https://doi.org/10.1016/j.vacuum.2017.07.030.

Tan, C., Tan, X., Shi, F., Yin, Y., Liu, G.-Q., Xiong, C., Wang, H., Luo, G., Yu, B., Noudem, J. G., Liang, B., & Jiang, J. (2021). Enhanced thermoelectric performance of p-type sintered BiSbTe-based composites with $AgSbTe_2$ addition. *Ceramics International*, *47*(1), 725-731. https://doi.org/10.1016/j.ceramint.2020.08.182

Thaowonkaew, S., Kumar, M., & Vora-ud, A. (2021). Thermoelectric properties of Ag-doped Sb_2Te_3 thin films on SiO_2 and polyimide substrates with rapid thermal annealing. *Journal of Electronic Materials*, *50*, 2669-2673. https://doi.org/10.1007/s11664-021-08788-w

Wang, Y., Liu, W.-D., Shi, X.-L., Hong, M., Wang, L.-J., Li, M., Wang, H., Zou, J., & Chen, Z.-G. (2020). Enhanced thermoelectric properties of nanostructured n-type Bi_2Te_3 by suppressing Te vacancy through non-equilibrium fast reaction. *Chemical Engineering Journal*, *391*, Article 123513. https://doi.org/10.1016/j.cej.2019.123513

Zhang, L., Shi, X.-L., Yang, Y.-L., & Chen, Z.-G. (2021). Flexible thermoelectric materials and devices: From materials to applications. *Materials Today*, *46*, 62-108. https://doi.org/10.1016/j.mattod.2021.02.016

Zheng, Z.-H., Fan, P., Luo, J.-T., Liang, G.-X., & Zhang, D.-P. (2013). Enhanced thermoelectric properties of antimony telluride thin films with preferred orientation prepared by sputtering a fan-shaped binary composite target. *Journal of Electronic Materials*, *42*(12), 3421-3425. https://doi.org/10.1007/s11664-013-2779-5

Zou, H., Rowe, D. M., & Min, G. (2001). Growth of p- and n-type bismuth telluride thin films by co-evaporation. *Journal of Crystal Growth*, *222*(1-2), 82-87. https://doi.org/10.1016/s0022-0248(00)00922-2